

Optimal vaccination strategies for a heterogenous population using multiple objectives: The case of L_1 – and L_2 –formulations

Fernando Saldaña^{*1}, Amira Kebir^{1,2,3}, José Ariel Camacho-Gutiérrez⁴ and Maíra Aguiar^{1,5,6}

¹*Basque Center for Applied Mathematics - BCAM, Bilbao, Spain*

²*IPEIT, Tunis University, Tunisia*

³*BIMS-IPT, Tunis El Manar University, Tunisia*

⁴*Facultad de Ciencias, Universidad Autónoma de Baja California, Baja California, Mexico*

⁵*Ikerbasque, Basque Foundation for Science, Bilbao, Spain*

⁶*Dipartimento di Matematica, Università degli Studi di Trento, Trento, Italy*

June 12, 2023

Abstract

The choice of the objective functional in optimization problems coming from biomedical and epidemiological applications plays a key role in optimal control outcomes. In this study, we investigate the role of the objective functional on the structure of the optimal control solution for an epidemic model that includes a core group with higher sexual activity levels than the rest of the population. An optimal control problem is formulated to find a targeted vaccination program able to control the spread of the infection with minimum vaccine deployment. Both L_1 – and L_2 –objectives are considered as an attempt to explore the trade-offs between control dynamics and the functional form characterizing optimality. Our results show that the optimal vaccination policy for both the L_1 – and the L_2 –formulation share one important qualitative property, that is, immunization of the core group should be prioritized by policymakers to achieve a fast reduction of the epidemic. Nevertheless, quantitative aspects of this result can be significantly affected depending on the objective weightings. Overall, our results suggest that the optimal control profiles are reasonably robust with respect to the L_1 – or L_2 –formulation when the monetary cost of the vaccination policy is substantially lower than the cost associated with the disease burden but if this is not the case the optimal control profiles can be radically different for each formulation.

Keywords: Optimal control, Mathematical modeling, Epidemic models, Vaccine allocation

1 Introduction

For a large number of infectious diseases, the presence of population heterogeneity, e.g. the existence of sub-populations with significant differences in mixing (contact) patterns and activity levels, can play an important role in disease spread and control [8, 34]. One key challenge for the control and prevention of infectious diseases is the optimal allocation of a limited vaccine supply in a heterogeneous population. In the uniform immunization program, the vaccine is administered at the same rate in all subgroups trying to reach herd immunity while keeping the vaccinated fraction as small as possible. Nevertheless, neglecting the heterogeneous properties of the population usually leads to inaccuracies in estimating the critical fraction that needs to be vaccinated to achieve disease eradication [8]. For an effective immunization program, it is critical to select subgroups that should receive priority for vaccination. In

^{*}Corresponding author: fsaldana@bcamath.org (Fernando Saldaña)

the context of sexually transmitted infections (STIs), targeted vaccination programs should consider the existence of a core group, a group of individuals with much higher rates of sexual activity. Core groups and their mixing with the general population have been shown to be epidemiologically relevant (see, for example, the seminal work [19]). Particularly, contact rates in the average population are often not sufficient for disease persistence. Instead, core groups are required to spread and maintain the disease in the entire population.

The optimal control theory (OCT) is an essential tool frequently used to solve a wide range of optimization problems for dynamical systems including vaccine allocation problems in public health [1, 4, 7, 9, 15, 17, 22, 27, 30, 35, 37, 41, 42, 45]. Probably one of the most relevant issues when solving optimization problems via OCT is the choice of the performance criterion, that is the objective functional to be minimized or maximized [11, 20, 16, 26, 43]. For medical and biological applications, the choice of such criterion is usually not straightforward. However, there is a vast amount of literature where the control cost is simply postulated to be proportional to a sum of the squares of the considered controls. These are the so-called L_2 -type functionals because they consider a weighted L_2 -norm on the control. This functional form has its origin in engineering applications where the square of the controls has a clear interpretation as the energy spent on the control action [16]. One important attribute of the L_2 -formulation is that it is amenable to mathematical analysis in the sense that the optimal control problem (OCP) can be reduced to a two-point boundary value problem which can be easily solved by standard numerical methods [22]. This mathematical convenience is probably the main reason that the L_2 -formulation is so widespread in the literature [4, 3, 5, 7, 15, 16, 20, 23, 26, 30, 35, 36, 45, 48]. Yet, for biomedical and epidemiological applications, the use of L_2 -objective functionals is frequently difficult to validate. For example, the authors in [26] have argued that for anticancer therapies, the financial control cost, including the costs of adverse side effects, is usually better approximated by a linear function of the magnitude of the corresponding control. In other words, a linear penalty term on the control, that is, an L_1 -type functional often leads to a more reasonable modeling of the cost. In [16] the authors also argued that the L_1 -formulation should be preferred over the L_2 -case to model control cost of mass vaccination campaigns in the context of infectious diseases. Nevertheless, there can be cases, for instance, if there is an overwhelmed healthcare system, where nonlinear forms of control cost are likely to occur. Still, a quadratic term is not necessarily the best modeling choice. Even if L_1 -objectives are, in general, more appropriate than the L_2 -ones for applications in biology, the L_1 -formulation of the OCP is usually challenging and involves the analysis of singular and bang-bang controls. In light of these issues, more attention should be paid to the appropriate selection of the objective functional and its impact on the optimal control solution.

In the present work, a multigroup Kermack-McKendrick-type model is proposed as a parsimonious approach to include population heterogeneity in the spread of an STI. Particular attention is given to the two-group case where the contact network only includes one non-core group and one core group. Contact patterns in the model consider preferential mixing as an improvement over the commonly used homogeneous mixing [14]. Two time-dependent vaccination rates are introduced, one for each group. The OCT is then used as a tool to develop an optimal immunization program for STIs that takes into account the presence of a core group within the population. The resulting targeted vaccination program will aim to control the spread of the infection by finding, for each group, the optimal vaccine allocation in terms of order and distribution, but at the same time minimizing the total vaccine deployment. To achieve this goal, we formulate an OCP that considers both L_1 - and L_2 -formulations to investigate how the objective impacts the resulting optimal control. It is important to remark that the qualitative analysis for different functionals is a nontrivial task by itself. Furthermore, since the value of the weight parameters in the objective function can play a significant role in the qualitative properties of the optimal control solutions [22, 26, 43], the impact of the weights on the solution is also investigated.

In the next section, we introduce the model, compute the basic reproduction number and prove that the model is epidemiologically well-posed. The analytical properties of the optimal control problems are discussed in Section 3. In the L_2 -formulation the control characterization is achieved using the Maximum Principle's first-order necessary conditions for optimality. In the L_1 -formulation, the study of singular arcs is investigated via the generalized Legendre-Clebsch condition. In Section 4, the analytical results from the previous sections are complemented with the numerical computation of the optimal control for a range of scenarios of interest. The discussion of our results is presented in Section 5.

2 A multigroup SIR-type model with time-dependent vaccination

In the general case, our system can be described by a SIR-type model in a population N divided into n mutually exclusive groups of size N_i ($i = 1, 2, \dots, n$) with heterogeneous sexual activity levels. Each group N_i is further divided according to infection status as susceptible (S_i), infectious (I_i), and immune individuals (R_i). The transmission dynamics of the system are governed by the following system of $3n$ ordinary differential equations (ODEs):

$$\begin{aligned}\frac{dS_i}{dt} &= \mu N_i - S_i \sum_{j=1}^n p a_i c_{ij} \frac{I_j}{N_j} - (u_i(t) + \mu) S_i + \alpha R_i, \\ \frac{dI_i}{dt} &= S_i \sum_{j=1}^n p a_i c_{ij} \frac{I_j}{N_j} - (\gamma + \mu) I_i, \\ \frac{dR_i}{dt} &= u_i(t) S_i + \gamma I_i - (\mu + \alpha) R_i,\end{aligned}\tag{1}$$

where all the parameters and initial conditions are nonnegative. Individuals are recruited into the susceptible class S_i of the group N_i at rate μ , assumed to be equal to the death rate, so each group has a constant population size N_i . After infection, individuals in class I_i recover naturally at a rate γ and move to the corresponding immune class R_i ($i = 1, 2, \dots, n$). Furthermore, immunization by a vaccine removes individuals from the susceptible class with a time-dependent vaccination rate $u_i(t)$. These individuals go the immune class R_i (natural and vaccine-induced immunity are assumed to act similarly). Loss of immunity occurs at a rate α proportional to the number of immune individuals, thus $1/(\alpha + \mu)$ is the average duration that people stay in the immune class. The acquisition of infection occurs with the force of infection given by

$$\sum_{j=1}^n p a_i c_{ij} \frac{I_j}{N_j}.\tag{2}$$

Here, p is the transmission probability per contact (assumed to be constant across groups), and a_i represents the average per capita contact rates of group i ($i = 1, 2, \dots, n$) i.e. sexual activity levels. The coefficients c_{ij} model the mixing among groups and are defined as the proportion of contacts that individuals in group i have with group j . The matrix $C = [(c_{ij})]$ is the mixing matrix or contact fraction matrix. A range of possible mixing patterns of sexual contacts with different degrees of assortative (within sexual activity groups) and disassortative (between sexual activity groups) mixing are possible [38]. We assume the so-called preferential mixing that was first introduced in [21], hence the elements of the contact fraction matrix are

$$c_{ij} = \epsilon_i \delta_{ij} + (1 - \epsilon_i) \frac{(1 - \epsilon_j) a_j N_j}{\sum_{k=1}^n (1 - \epsilon_k) a_k N_k}, \quad i, j = 1, 2, \dots, n\tag{3}$$

where ϵ_i is the fraction of within-group i contacts also called preference level of group i , and δ_{ij} is the Kronecker delta ($\delta_{ij} = 1$ when $i = j$ and $\delta_{ij} = 0$ otherwise). The coefficients c_{ij} given by (3) satisfy the constraints for mixing functions particularly $a_i N_i c_{ij} = a_j N_j c_{ji}$ ($i, j = 1, 2, \dots, n$) [14].

In this study, we are interested in a particular case of model (1) that considers only two groups. The size of group N_1 is assumed to be way bigger than that of the group N_2 , hence $N_1 = (1 - f)N$, and $N_2 = fN$ with $0 < f \ll 1$ being the fraction of the population that belongs to the core group. Group N_1 is characterized by a low sexual activity level in comparison with the activity level of group N_2 , thus $a_1 < a_2$. In other words, group N_2 constitutes a core group within the population, so individuals in this group have high levels of sexual activity, and hence may be more likely to acquire and transmit the infection. A high degree of assortative mixing is also assumed so within-group contacts are stronger than between-group contacts. Therefore, $0.5 < \epsilon_i < 1$ ($i = 1, 2$). Under these conditions the two-group

model is defined by the following system:

$$\begin{aligned}
\frac{dS_1}{dt} &= \mu N_1 - \left(c_{11} \frac{I_1}{N_1} + c_{12} \frac{I_2}{N_2} \right) p a_1 S_1 - (u_1(t) + \mu) S_1 + \alpha R_1, \\
\frac{dI_1}{dt} &= \left(c_{11} \frac{I_1}{N_1} + c_{12} \frac{I_2}{N_2} \right) p a_1 S_1 - (\gamma + \mu) I_1, \\
\frac{dR_1}{dt} &= u_1(t) S_1 + \gamma I_1 - (\mu + \alpha) R_1, \\
\frac{dS_2}{dt} &= \mu N_2 - \left(c_{21} \frac{I_1}{N_1} + c_{22} \frac{I_2}{N_2} \right) p a_2 S_2 - (u_2(t) + \mu) S_2 + \alpha R_2, \\
\frac{dI_2}{dt} &= \left(c_{21} \frac{I_1}{N_1} + c_{22} \frac{I_2}{N_2} \right) p a_2 S_2 - (\gamma + \mu) I_2, \\
\frac{dR_2}{dt} &= u_2(t) S_2 + \gamma I_2 - (\mu + \alpha) R_2,
\end{aligned} \tag{4}$$

subject to non-negative initial conditions

$$S_i(0) = S_{i0} > 0, I_i(0) = I_{i0} > 0, R_i(0) = R_{i0} \geq 0, S_{i0} + I_{i0} + R_{i0} = N_i, (i = 1, 2). \tag{5}$$

Baseline parameter values for system (4) are summarized in Table 1. Mean values for some of the model parameters are obtained using sexual behavior data from [28] and estimations from previous studies of STIs (see [13, 18, 35] and the references therein). Instead of focusing on a single disease, we consider a set of scenarios of interest that are feasible for the most frequent STIs. Furthermore, since in the case of sub-critical dynamics, the use of control is not appealing, contact rates are adjusted to produce super-critical epidemiological dynamics. The core group is assumed to be three times more active in terms of per capita contact rate than the non-core group (see Table 1).

In model (4), $u_1(t)$ and $u_2(t)$ are time-dependent vaccination rates for the low-risk (N_1) and high-risk (N_2) groups, respectively, and will be called controls. Due to logistic limitations, under any realistic scenario, these vaccination rates should be constrained under a maximum vaccination rate u_{max} per unit of time e.g. daily vaccination rate. As shown in [35], a vaccination rate u can be approximated by $u = -\ln(1 - C(\tau))/\tau$ where $C(\tau)$ is the immunization coverage at time τ . We consider a case in which health authorities can achieve a vaccination coverage $C(\tau) = 80\%$ of the population in one year ($\tau = 365$ days), then the vaccination rate is equal to $u \approx 1.60/365$ per day. Therefore, the vaccination rates are subject to constraints

$$u_1(t), u_2(t) \in [0, u_{max}], \quad u_{max} = 1.60/365 \approx 0.0043. \tag{6}$$

We are interested in studying the dynamics of model (4) over a finite time interval $[0, t_f]$. Furthermore, if the initial number of infected individuals is zero, then the infectious classes remain with zero individuals during the whole time period. Therefore, in an epidemiologically appealing case, one needs to consider positive initial conditions for the susceptible and infectious classes. Let us define the state vector as $X = (S_1, I_1, R_1, S_2, I_2, R_2)$, then the biologically feasible region for system (4) is

$$\Omega = \{X \in \mathbf{R}_+^6 : N_i = S_i(t) + I_i(t) + R_i(t) > 0, S_i(t) > 0, I_i(t) > 0, R_i(t) \geq 0; t \in [0, t_f] (i = 1, 2)\}.$$

The set of admissible controls $D_0(t_f)$ is defined as the set of all possible Lebesgue-measurable functions $U = (u_1(t), u_2(t))$, which satisfy conditions (6) for almost all $t \in [0, t_f]$.

Let $X_0 = (S_{10}, I_{10}, R_{10}, S_{20}, I_{20}, R_{20}) \in \Omega$, and $U(t) \in D_0(t_f)$. Observe that model equations for the infectious classes in (4) present the equilibrium solution $I_1(t) = I_2(t) = 0$, and hence if $I_{10}, I_{20} > 0$, as long as the solution exists, the infected classes $I_1(t)$ and $I_2(t)$ will remain positive. If $S_i(0) = S_{i0} > 0$ ($i = 1, 2$), define $t_1 = \inf\{t > 0 : S_i(t) = 0\}$. If t_1 is finite, then $S_i(t_1) = 0$ implies $\dot{S}_i(t_1) = \mu N_i + \alpha R_i(t_1) > 0$, which is a contradiction so $S_i(t)$ remains positive for all $t \in [0, t_f]$. Likewise, if $R_i(t) = 0$, then $\dot{R}_i(t) > 0$ for all $t \in [0, t_f]$, therefore R_i ($i = 1, 2$) will remain nonnegative. Hence, if the initial condition satisfies $X_0 \in \Omega$, then the solution of model (4) cannot leave the region Ω in forward time. This is summarized in the following result.

Proposition 1. *Consider an initial condition for model (4) such that $X_0 \in \Omega$ is satisfied. Then for any admissible controls $U(t) \in D_0(t_f)$, the corresponding solution $X(t)$ exists and remains in Ω for all $t \in [0, t_f]$.*

Therefore the region Ω is a positively invariant set under the flow of model (4) and the system is epidemiologically well-posed. Stability properties for the equilibrium points of system (1) in the no-control case (i.e. with $u_1(t) = u_2(t) = 0$ for all t) have been discussed in previous studies [21] showing that: (i) if $R_0 < 1$, then system (1) has a unique disease-free equilibrium which is globally asymptotically stable so the disease dies out, and (ii) if $R_0 > 1$, then there exists an endemic equilibrium that is globally asymptotically stable thus the disease persists in the population. In the case of the 2-group model (4), the basic reproduction number R_0 can be obtained as the spectral radius of the next-generation matrix

$$\mathbf{K} = \begin{bmatrix} \frac{pa_1c_{11}}{\gamma + \mu} & \frac{pa_1c_{12}}{\gamma + \mu} \frac{N_1}{N_2} \\ \frac{pa_2c_{21}}{\gamma + \mu} \frac{N_2}{N_1} & \frac{pa_2c_{22}}{\gamma + \mu} \end{bmatrix}.$$

The analytical expression for R_0 is

$$R_0 = \frac{1}{2} \frac{p}{\gamma + \mu} \left(a_1c_{11} + a_2c_{22} + \sqrt{(a_1c_{11} - a_2c_{22})^2 + 4a_1a_2c_{12}c_{21}} \right). \quad (7)$$

It is easy to see that R_0 is an increasing function of the transmission probability per contact p and the average per capita contact rates a_i ($i = 1, 2$). Furthermore, observing that $N_1/N_2 = (1 - f)/f > 1$ and $N_2/N_1 = f/(1 - f) < 1$, a direct computation can show that $\partial R_0/\partial f > 0$ so the value of R_0 increases as the fraction f in the core group increases (see Figure 1(a)). The case of super-critical epidemiological dynamics ($R_0 = 2.09 > 1$) is shown in Figure 1(b).

Parameters	Mean value – Range
Sexually active life expectancy ($1/\mu$)	50 – (30, 60) <i>year</i>
Average per capita contact rate of group 1 (a_1)	30 – (0, 100) <i>year</i> ⁻¹
Average per capita contact rate of group 2 (a_2)	90 – (0, 100) <i>year</i> ⁻¹
Transmission probability per contact (p)	0.50 – (0, 1)
Fraction of within-group 1 contacts (ϵ_1)	0.80 – (0, 1)
Fraction of within-group 2 contacts (ϵ_2)	0.60 – (0, 1)
Fraction of individuals that belong to the core group N_2 (f)	0.20 – (0, 0.5)
Recovery rate (α)	1/365 – (1/3650, 1/30) <i>days</i>
Duration of the infectious period ($1/\gamma$)	20 – (10, 100) <i>days</i>
Vaccination rates u_i ($i = 1, 2$)	0.50 – (0.0, 1.60) <i>year</i> ⁻¹

Table 1: Baseline parameters for model (4). Observe that the values for the coefficients c_{ij} are obtained via their definition (3) substituting the values of the parameters a_i , ϵ_i , and N_i ($i = 1, 2$). The total population is assumed to be $N = 100000$.

3 Insights from optimal control theory

Here, we use OCT as a tool to develop an optimal immunization program for STIs that takes into account the presence of a core group within the population. The resulting targeted vaccination program will aim to control the spread of the infection while trying to minimize the total vaccine deployment.

A key issue when solving optimization problems in biological applications via OCT is the choice of the objective functional to be minimized or maximized [11, 16, 20, 26, 43]. In the context of epidemiological applications, the objective functional typically falls into the following general form e.g. [3, 4, 5, 7, 15, 23, 30, 35, 36, 44, 45, 48]:

$$J(U) = \int_0^{t_f} L(X(t)) + \sigma(U(t)) dt. \quad (8)$$

Here L is a function that allows the minimization of undesirable state variables. For epidemiological models, one often needs to minimize the prevalence of the infection, so L is assumed to be proportional

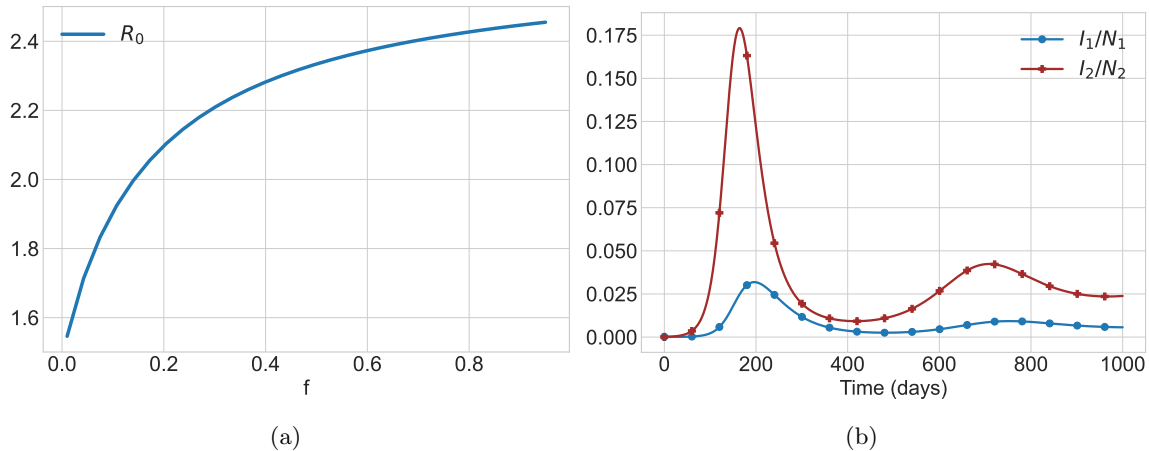


Figure 1: (a) The basic reproduction number as a function of the fraction f of individuals that belong to the core group N_2 . (b) Super-critical dynamics for the fraction I_i/N_i of infected individuals in each group ($i = 1, 2$). Model parameters are taken from Table 1.

to the infectious class. The function σ aims to optimize the use of the control. An objective of the form (8) has as a main goal minimization of the disease burden but also the use of control. We remark that alternative formulations can also be found in the literature, for instance, using an isoperimetric constraint to model a specific health budget or minimum-time control problems [1, 20, 37] but these examples are relatively uncommon, and the majority of OC studies in epidemiology use an objective within the general form (8).

The function $\sigma(U(t))$ in (8) is usually defined as $\sigma(U) = \sum_j B_j u_j^k(t)$ with $k = 1$ or $k = 2$, hence, the control cost is a weighted L_1 - or L_2 -norm, respectively. The choice of L_1 - or L_2 -norm in $\sigma(U(t))$ is not inconsequential and is a source of constant controversy [16, 26]. The issue is that in the majority of biological applications, the actual form of the costs and the dependency on these controls are subject to the modeler's interpretation and can barely be defined with an acceptable degree of accuracy. We consider both L_1 - and L_2 -objective functionals as an attempt to explore the trade-offs between control dynamics and the functional form characterizing optimality. To this end, we propose the next objective functional:

$$J_k(U) = \int_0^{t_f} A_1 \frac{I_1(t)}{N_1} + A_2 \frac{I_2(t)}{N_2} + B_{1,k} u_1^k(t) + B_{2,k} u_2^k(t) dt \quad (k = 1, 2). \quad (9)$$

The OCP is to minimize the objective functional $J_k(U)$ over the set of admissible controls $U(t) \in D_0(t_f)$ subject to the dynamics of the model (4). The weight parameters $A_i > 0$ and $B_{i,k} > 0$ ($i, k = 1, 2$) are meaningful variables of choice to balance the impact of the presence of infected individuals and the use of control. The value of the weights can play a significant role in the qualitative properties of the optimal control solutions and hence should be calibrated with care to obtain meaningful results. An appropriate weighting is particularly relevant when considering both linear and quadratic control terms. For example, in model (4) the vaccination rates satisfy $0 \leq u_i^2 \leq u_i \leq u_{max} < 1$ ($i = 1, 2$), so in this case L_1 -cost is proportionally more penalising than L_2 -cost. Therefore, to make a fair comparison between formulations, we allow the weights $B_{i,k}$ ($i, k = 1, 2$) to vary depending on the control norm chosen.

3.1 The existence of the optimal control

The existence of the optimal control comes as a direct result of Theorem 4.1 in [12, Chapter III]. The result is formalized as follows.

Theorem 1. *Consider the objective functional (9) subject to model dynamics (4) with the initial conditions (5). Then there exists an optimal pair of controls $U^* = (u_1^*, u_2^*)$ and a corresponding optimal state X^* that minimizes the objective function $J_k(U)$ over set of admissible controls $D_0(t_f)$ for all $k \in \{1, 2\}$.*

Proof. The following assertions are verified:

- (A1) *The set of controls and corresponding state variables is nonempty.* Since the set of admissible controls $D_0(t_f)$ and the right-hand side of model (4) is bounded, the Carathéodory Theorem [29, Chapter IX, Theorem 9.2.1] ensures that the set of admissible state variables and control variables is not empty.
- (A2) *The admissible control set $D_0(t_f)$ is convex and closed.* Observe that $D_0(t_f)$ is closed and convex by definition.
- (A3) *The right-hand side of the state system (4) is bounded by a linear function in states and control variables.* This follows from the fact that the right-hand side of model (4) is linear in the controls and the solution of (4) is bounded.
- (A4) *The integrand of the objective functional $\mathcal{L}_k(X, U) = L(X) + \sigma(U)$ is convex on the set $D_0(t_f)$.* Observe that the Hessian matrix of \mathcal{L}_k for all $k \in \{1, 2\}$ as function of the control is positive semi-definite on $D_0(t_f)$.
- (A5) *There exists constants $\omega_1 > 0$, ω_2 and $\rho > 1$, such that:*

$$\mathcal{L}_k(X, U) \geq \omega_1 \|(u_1, u_2)\|^\rho - \omega_2, \forall k \in \{1, 2\}. \quad (10)$$

According to Proposition 1, $\|X\| > 0$. Moreover, bounds (6) state that $0 \leq u_1, u_2 \leq u_{max} < 1$ so $u_1 \geq u_1^2$ and $u_2 \geq u_2^2$. Therefore, for all $k \in \{1, 2\}$,

$$\mathcal{L}_k(X, U) \geq \sigma(U) \geq \min(B_{1,k}, B_{2,k})(u_1^2 + u_2^2)$$

Hence, choosing $\omega_1 = \min(B_{1,k}, B_{2,k}) > 0$, $\omega_2 = 0$ and $\rho = 2 > 1$, condition (10) is satisfied.

3.2 Necessary conditions via the Maximum Principle

We obtain the necessary conditions for optimality of a controlled trajectory (X^*, U^*) via the Maximum Principle. To this end, we consider the control Hamiltonian H_k defined as follows

$$H_k(X(t), U(t), \lambda(t), \lambda_0) = \lambda_0 \left(A_1 \frac{I_1(t)}{N_1} + A_2 \frac{I_2(t)}{N_2} + B_{1,k} u_1^k(t) + B_{2,k} u_2^k(t) \right) + \langle \lambda(t), \Phi(X(t), U(t)) \rangle \quad (11)$$

where $\Phi(X(t), U(t))$ is the right-hand side of model (4), so $X'(t) = \Phi(X(t), U(t))$ and $\langle \cdot, \cdot \rangle$ denotes the usual dot product. The multiplier λ_0 is a non-negative constant and $\lambda(t) = (\lambda_1(t), \dots, \lambda_6(t))$ are piecewise differentiable adjoint variables which have a classical interpretation in OCP as the marginal valuation of the associated state variable at time t [22]. We write H_k to remark the explicit dependence on k for the Hamiltonian. The Maximum Principle converts the OCP into a problem of minimizing pointwise the Hamiltonian over the set of admissible controls $U(t) \in D_0(t_f)$ along the optimal controlled trajectory $X^*(t)$, hence

$$H_k(X^*(t), U^*(t), \lambda(t), \lambda_0) \leq H_k(X^*(t), U(t), \lambda(t), \lambda_0), \quad \forall U(t) \in D_0(t_f), \quad (12)$$

and $H_k(X^*(t), U^*(t), \lambda(t), \lambda_0) = const$, so the Hamiltonian is constant with minimum value along the optimal solution. Furthermore, the co-states $\lambda_i(t)$ ($i = 1, \dots, 6$) satisfy the following adjoint system

$$\frac{d\lambda_i}{dt} = - \frac{\partial H_k(X^*(t), U^*(t), \lambda(t), \lambda_0)}{\partial X_i}, \quad \lambda_i(t_f) = 0. \quad (13)$$

The explicit adjoint system is thus as follows

$$\begin{aligned}
\frac{d\lambda_1}{dt} &= \lambda_1 \left[\left(c_{11} \frac{I_1}{N_1} + c_{12} \frac{I_2}{N_2} \right) pa_1 + (u_1(t) + \mu) \right] - \lambda_2 \left(c_{11} \frac{I_1}{N_1} + c_{12} \frac{I_2}{N_2} \right) pa_1 - \lambda_3 u_1(t), \\
\frac{d\lambda_2}{dt} &= -\lambda_0 \frac{A_1}{N_1} + \lambda_1 c_{11} pa_1 \frac{S_1}{N_1} - \lambda_2 \left(c_{11} pa_1 \frac{S_1}{N_1} - (\gamma + \mu) \right) - \lambda_3 \gamma + (\lambda_4 - \lambda_5) c_{21} pa_2 \frac{S_2}{N_1}, \\
\frac{d\lambda_3}{dt} &= -\lambda_1 \alpha + \lambda_3 (\mu + \alpha), \\
\frac{d\lambda_4}{dt} &= \lambda_4 \left[\left(c_{21} \frac{I_1}{N_1} + c_{22} \frac{I_2}{N_2} \right) pa_2 + (u_2(t) + \mu) \right] - \lambda_5 \left(c_{21} \frac{I_1}{N_1} + c_{22} \frac{I_2}{N_2} \right) pa_2 - \lambda_6 u_2(t), \\
\frac{d\lambda_5}{dt} &= -\lambda_0 \frac{A_2}{N_2} + (\lambda_1 - \lambda_2) c_{12} pa_1 \frac{S_1}{N_2} + \lambda_4 c_{22} pa_2 \frac{S_2}{N_2} - \lambda_5 \left(c_{22} pa_2 \frac{S_2}{N_2} - (\gamma + \mu) \right) - \lambda_6 \gamma, \\
\frac{d\lambda_6}{dt} &= -\lambda_4 \alpha + \lambda_6 (\mu + \alpha),
\end{aligned} \tag{14}$$

subject to the terminal condition $\lambda_i(t_f) = 0$ for $i = 1, 2, \dots, 6$.

From the Maximum Principle it follows that λ_0 and $\lambda(t)$ do not vanish simultaneously for an optimal pair $(X^*(t), U^*(t))$. Therefore, the terminal condition in (13) implies that $\lambda_0 > 0$. Normal extremals are considered assuming $\lambda_0 = 1$ [25]. Hence, λ_0 will be omitted in the notation subsequently. Since the Hamiltonian (11) is affine in the controls and the control set is compact, the minimum conditions break into separate scalar minimization problems via the functions

$$\psi_{i,k}(t) = \frac{\partial H_k(X^*(t), U^*(t), \lambda(t))}{\partial U_i}, \quad (i, k = 1, 2). \tag{15}$$

The first-order optimality condition $\psi_{i,k}(t) = 0$, must be satisfied so the Hamiltonian has a minimum in the set of admissible controls. The epidemic model (4) and the adjoint system (14) constitute a two-point boundary value problem that is coupled with the OCP via the optimality condition.

3.2.1 The case of an L_2 -objective functional

In the case of an L_2 -objective functional ($k = 2$), the first-order optimality condition can be used to obtain the control characterization as follows

$$\begin{aligned}
\psi_{1,2}(t) &= \frac{\partial H_2(X^*(t), U^*(t), \lambda(t))}{\partial u_1} = 2B_{1,2}u_1^*(t) - \lambda_1(t)S_1^*(t) + \lambda_3(t)S_1^*(t) = 0, \\
\psi_{2,2}(t) &= \frac{\partial H_2(X^*(t), U^*(t), \lambda(t))}{\partial u_2} = 2B_{2,2}u_2^*(t) - \lambda_4(t)S_2^*(t) + \lambda_6(t)S_2^*(t) = 0.
\end{aligned} \tag{16}$$

Considering the lower and upper bounds for the controls and the optimality condition (16), we obtain the following characterization of the optimal controls:

$$u_{1,2}^*(t) = \min \left\{ \max \left\{ 0, \frac{(\lambda_1(t) - \lambda_3(t))S_1^*(t)}{2B_{1,2}} \right\}, u_{max} \right\}, \tag{17}$$

$$u_{2,2}^*(t) = \min \left\{ \max \left\{ 0, \frac{(\lambda_4(t) - \lambda_6(t))S_2^*(t)}{2B_{2,2}} \right\}, u_{max} \right\}. \tag{18}$$

3.2.2 The case of an L_1 -objective functional

Now, the case of an L_1 -objective functional is considered ($k = 1$). Under these conditions, the $\psi_{i,1}$ ($i = 1, 2$) functions are known as switching functions because if these functions are different from zero, the optimal controls satisfy

$$u_{i,1}^*(t) = \begin{cases} 0, & \psi_{i,1}(t) > 0 \\ u_{max}, & \psi_{i,1}(t) < 0 \end{cases} \tag{19}$$

where

$$\begin{aligned}
\psi_{1,1}(t) &= B_{1,1} - (\lambda_1(t) - \lambda_3(t))S_1(t), \\
\psi_{2,1}(t) &= B_{2,1} - (\lambda_4(t) - \lambda_6(t))S_2(t).
\end{aligned} \tag{20}$$

Observe that in the L_1 -case, the optimality condition $\psi_{i,1} = 0$ ($i = 1, 2$) does not depend on the control functions and hence we cannot directly obtain the control characterization. The bang-bang solution of the problem is (19), nevertheless, if

$$\psi_{i,1}(t) = 0, \quad t \in I_i \subset [0, t_f] \quad (i = 1, 2) \quad (21)$$

where $I_i \subset [0, t_f]$ is an open interval, then singular controls and arcs can appear [6, 10, 17]. Let us assume that (21) holds to investigate the singular solution. First, observe that $\psi_{1,1}(t) = 0$ implies that

$$\lambda_1(t) - \lambda_3(t) = B_{1,1}/S_1(t) > 0. \quad (22)$$

In the singular interval I_1 the first and second derivatives of $\psi_{1,1}(t)$ also vanish, hence using the chain rule

$$\begin{aligned} 0 &= \frac{d\psi_{1,1}}{dt} = S_1 \left(\frac{d\lambda_3}{dt} - \frac{d\lambda_1}{dt} \right) + (\lambda_3 - \lambda_1) \frac{dS_1}{dt} = \\ &S_1 \left(-\lambda_1 \left[\left(c_{11} \frac{I_1}{N_1} + c_{12} \frac{I_2}{N_2} \right) pa_1 + (u_1(t) + \mu + \alpha) \right] + \lambda_2 \left(c_{11} \frac{I_1}{N_1} + c_{12} \frac{I_2}{N_2} \right) pa_1 + \lambda_3 (u_1(t) + \mu + \alpha) \right) \\ &+ (\lambda_3 - \lambda_1) \left(\mu N_1 - \left(c_{11} \frac{I_1}{N_1} + c_{12} \frac{I_2}{N_2} \right) pa_1 S_1 - (u_1(t) + \mu) S_1 + \alpha R_1 \right) = \\ &S_1 (\lambda_2 - \lambda_3) \left(c_{11} \frac{I_1}{N_1} + c_{12} \frac{I_2}{N_2} \right) pa_1 + (\lambda_3 - \lambda_1) (\mu N_1 + \alpha R_1) - \alpha B_{1,1} \end{aligned}$$

Solving for $\lambda_2 - \lambda_3$ in the above equation:

$$(\lambda_2 - \lambda_3) S_1 pa_1 \left(c_{11} \frac{I_1}{N_1} + c_{12} \frac{I_2}{N_2} \right) = (\lambda_1 - \lambda_3) (\mu N_1 + \alpha R_1) + \alpha B_{1,1} > 0. \quad (23)$$

Lengthy computations allow us to obtain $\frac{d^2\psi_{1,1}}{dt^2} = F_1(X, \lambda) + G_1(X, \lambda)u_1$ where the functions $F_1(X, \lambda)$ and $G_1(X, \lambda)$ depend only on states and adjoint variables (and model parameters). As a consequence,

$$\frac{\partial}{\partial u_1} \frac{d^2\psi_{1,1}}{dt^2} = G_1(X, \lambda) = (\lambda_3 - \lambda_1) (\mu N_1 + \alpha R_1) - \alpha B_{1,1} + S_1 pa_1 (\lambda_3 - \lambda_2) \left(c_{11} \frac{I_1}{N_1} + c_{12} \frac{I_2}{N_2} \right).$$

Using the expressions (22) and (23) we get

$$-\frac{\partial}{\partial u_1} \frac{d^2\psi_{1,1}}{dt^2} = 2[(\lambda_1 - \lambda_3) (\mu N_1 + \alpha R_1) + \alpha B_{1,1}] > 0.$$

Analogous computations show that $\frac{d^2\psi_{2,1}}{dt^2} = F_2(X, \lambda) + G_2(X, \lambda)u_2$ and $-\frac{\partial}{\partial u_2} \frac{d^2\psi_{2,1}}{dt^2} > 0$. Therefore, the order of the singularity κ_i of control u_i is $\kappa_i = 1$ ($i = 1, 2$) [10].

The generalized Legendre-Clebsch conditions [10, 24] state that if controls u_1, u_2 are singular of order 1 on an interval I , then the matrix M whose entries are given by

$$M_{i,j} = (-1) \frac{\partial}{\partial u_i} \frac{d^2}{dt^2} \frac{\partial H_1}{\partial u_j} = -\frac{\partial}{\partial u_i} \frac{d^2\psi_{j,1}}{dt^2}, \quad (i, j = 1, 2)$$

must be non-negative definite for the control to be minimizing. For our model, the non-diagonal entries of the above matrix satisfy

$$M_{1,2} = -\frac{\partial}{\partial u_1} \frac{d^2\psi_{2,1}}{dt^2} = 0, \quad M_{2,1} = -\frac{\partial}{\partial u_2} \frac{d^2\psi_{1,1}}{dt^2} = 0.$$

Hence, the Legendre-Clebsch condition implies that $M_{1,1} = -\frac{\partial}{\partial u_1} \frac{d^2\psi_{1,1}}{dt^2}$ and $M_{2,2} = -\frac{\partial}{\partial u_2} \frac{d^2\psi_{2,1}}{dt^2}$ should be greater or equal to zero, which is true in our case with strict inequality.

Since the generalized Legendre-Clebsch condition holds we can solve $\frac{d^2\psi_{1,1}}{dt^2} = 0$ with respect to the control variable $u_1(t)$ to get its singular part, getting

$$u_{1,sing} = \frac{f_1(X, \lambda)}{g_1(X, \lambda)},$$

where

$$\begin{aligned} f_1(X, \lambda) = & (N_1N_2c_{12}I_2 + N_2^2c_{11}I_1)(a_2c_{21}pS_2(\lambda_4 - \lambda_5) - A_1)pa_1S_1 \\ & + (N_1^2N_2^2\alpha^2(R_1 + S_1 + \gamma I_1) + N_1^3N_2^2(2\alpha\mu + \mu^2) - a_1^2c_{11}p^2N_2S_1^2(N_1c_{12}I_2 + N_2c_{11}I_1))(\lambda_3 - \lambda_1) \\ & + a_1pN_1(N_1N_2c_{12}I_2 + N_2^2c_{11}I_1)\{(\mu N_1 + \alpha R_1)(\lambda_1 - 2\lambda_2 + \lambda_3) + \alpha S_1(\lambda_1 + \lambda_2 - 2\lambda_3) + \mu S_1(\lambda_3 - \lambda_2)\} \\ & + \{a_1(N_1c_{12}I_2 + N_2c_{11}I_1)^2 - a_2c_{12}N_1S_2(N_1c_{22}I_2 + N_2c_{21}I_1)\}a_1p^2S_1(\lambda_3 - \lambda_2) \end{aligned}$$

and

$$g_1(X, \lambda) = N_1N_2([N_1\mu + \alpha(R_1 + S_1)]N_1N_2(\lambda_1 - \lambda_3) + (N_1c_{12}I_2 + N_2c_{11}I_1)a_1pS_1(\lambda_2 - \lambda_3))$$

Observe that the inequalities (22) and (23) imply that $g_1(X, \lambda)$ is never zero in all $t \in [0, t_f]$. A similar analysis can be used to obtain the singular part $u_{2,sing}(t)$.

4 Numerical results

In the case of the L_2 -formulation, the standard forward-backward sweep method (FBSM) algorithm can be used to obtain numerical approximations of the optimal control solution [27]. Nevertheless, in the L_1 -formulation the presence of singular arcs may cause convergence problems for the FBSM [27, 26]. Here, the numerical solution to the OCP is obtained by employing a large-scale nonlinear programming method called IPOPT (short for Interior Point OPTimizer) that implements an interior-point algorithm with a filter line-search method [46]. It is important to remark that, a priori, there is no guarantee that a numerical approximation of the control is optimal as only extremals are obtained [26]. For the L_2 -formulation, sufficient conditions for strong local optimality can be verified by addressing the issue of conjugate points as developed in [39].

Several numerical scenarios are investigated to evaluate the impact of the form of the dependency of the objective functional on the considered controls (L_2 - or L_1 -norm). It is important to remark that the parameters A_i and $B_{i,k}$ ($i, k = 1, 2$) are meaningful variables of choice to weigh the relative contribution of each term in the objective functional. For example, if the control weights $B_{i,k}$ ($i = 1, 2$) are too high the costs of the intervention usually limit in excess the use of control, and no vaccines will be given. On the other hand, if the value of the control weights is too low, it is expected that the optimal control would suggest the use of control at the maximum rate for long periods of time. Furthermore, when considering both linear and quadratic control terms, extra care should be put to select appropriate weights. For instance, in model (4) the vaccination rates satisfy $0 \leq u_i^2 \leq u_i \leq u_{max} < 1$ ($i = 1, 2$), therefore, in this case L_1 -cost is proportionally more penalising than L_2 -cost.

For the sake of clarity, in the numerical experiments, it is assumed that the cost of having infected individuals is the same for both the non-core and core group. This implies that $A_1 = A_2 > 0$. Likewise, it is assumed that $B_{1,k} = B_{2,k} > 0$ ($k = 1, 2$) so for all cases, the cost of using vaccines is also the same for both groups. This is a realistic assumption since the cost of vaccines does not depend on the level of sexual activity. Under these conditions, minimization of the objective functional (9) is equivalent to minimize

$$\tilde{J}_k(U) = \int_0^{t_f} \frac{I_1(t)}{N_1} + \frac{I_2(t)}{N_2} + W_k(u_1^k(t) + u_2^k(t)) dt, \quad (k = 1, 2) \quad (24)$$

where W_k ($k = 1, 2$) is a positive parameter. One critical observation is that the terms u_i^k in (24) lie in the intervals $[0, u_{max}]$ and $[0, u_{max}^2]$ with $u_{max} \approx 0.0043$ and $u_{max}^2 \approx 0.000018$ for $k = 1$ and $k = 2$, respectively. Therefore, one way to have a fair comparison between the L_1 - and L_2 -formulations is to calibrate the weights such that the maximum cost for both formulations is approximately the same. For our model parameters, one can assume $240W_1 = W_2$ so

$$W_1u_{max} \approx W_2u_{max}^2. \quad (25)$$

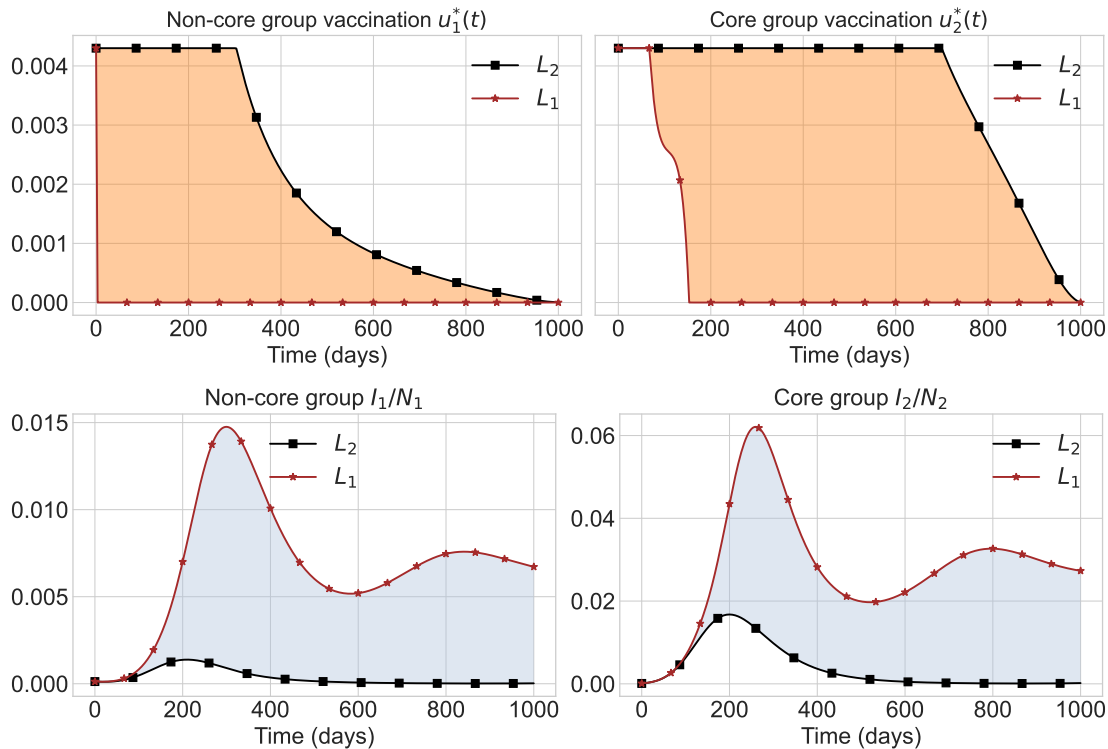


Figure 2: (First row) Vaccination rates $u_1^*(t)$ (first column) and $u_2^*(t)$ (second column) for the non-core group and the core group, respectively. (Second row) Associated controlled infectious classes. The shaded area illustrates the difference between the L_2 - and L_1 -formulations. The weights are fixed as $W_1 = W_2 = 15$.

We need to remark that if the weights are chosen independently of the control formulation in the objective, then the quantitative properties of the solution of the OCP can differ considerably between the formulations. An illustrative example of this scenario is shown in Figure 2 where the weights are chosen equally for both formulations $W_1 = W_2 = 15$. The numerical approximation for the optimal control profiles and the associated infectious classes are shown in the first and second rows in Figure 2, respectively. Each plot presents the solution for both the L_1 - and the L_2 -formulation and the shaded area illustrates the difference between formulations. Observe that the optimal vaccination rates in the L_2 - are radically higher than in the L_1 -case. In quantitative terms, the optimal vaccination rate for the core group $u_2^*(t)$ should be maintained at the maximum rate for approximately 700 days for the L_2 -formulation and less than 100 days for the L_1 -formulation. For the optimal vaccination rate of the non-core group $u_1^*(t)$, the maximum rate should be given for more than 300 days in the L_2 -formulation but this rate should be zero in the whole time horizon for the L_1 -formulation. As a consequence, the prevalence levels are substantially lower for the L_2 -formulation (see Figure 2).

Now we propose the following three scenarios for the weights such that (25) is fulfilled:

$$(I) W_1 = 0.1, W_2 = 24, \quad (II) W_1 = 1, W_2 = 240, \quad (III) W_1 = 30, W_2 = 7200 \quad (26)$$

Observe that the fractions I_i/N_i in the objective functional (24) lie, by definition, between zero and one; yet, for our parameter values the maximum peak size is below 0.2 (see Figure 1(b)) so $I_i/N_i \in [0, 0.2)$ ($i = 1, 2$). Hence, scenario (I) implies that the maximum cost of the vaccination program is significantly less expensive than the maximum cost of infection, whereas in scenario (II) the cost of vaccines is just a bit less expensive than the cost of infection, and in (III) both costs are of similar magnitudes. The numerical approximation for the optimal control profiles is shown in Figure 3. Row i shows the solution for Case i ($i = I, II, III$).

In case I (first row in Figure 3), the control profiles for the L_1 -solution follow a bang structure where the vaccination rate for the core group should be maintained for approximately 800 days and almost 400 days for the non-core group. The control profiles for the L_2 -solution maintain the maximum rates

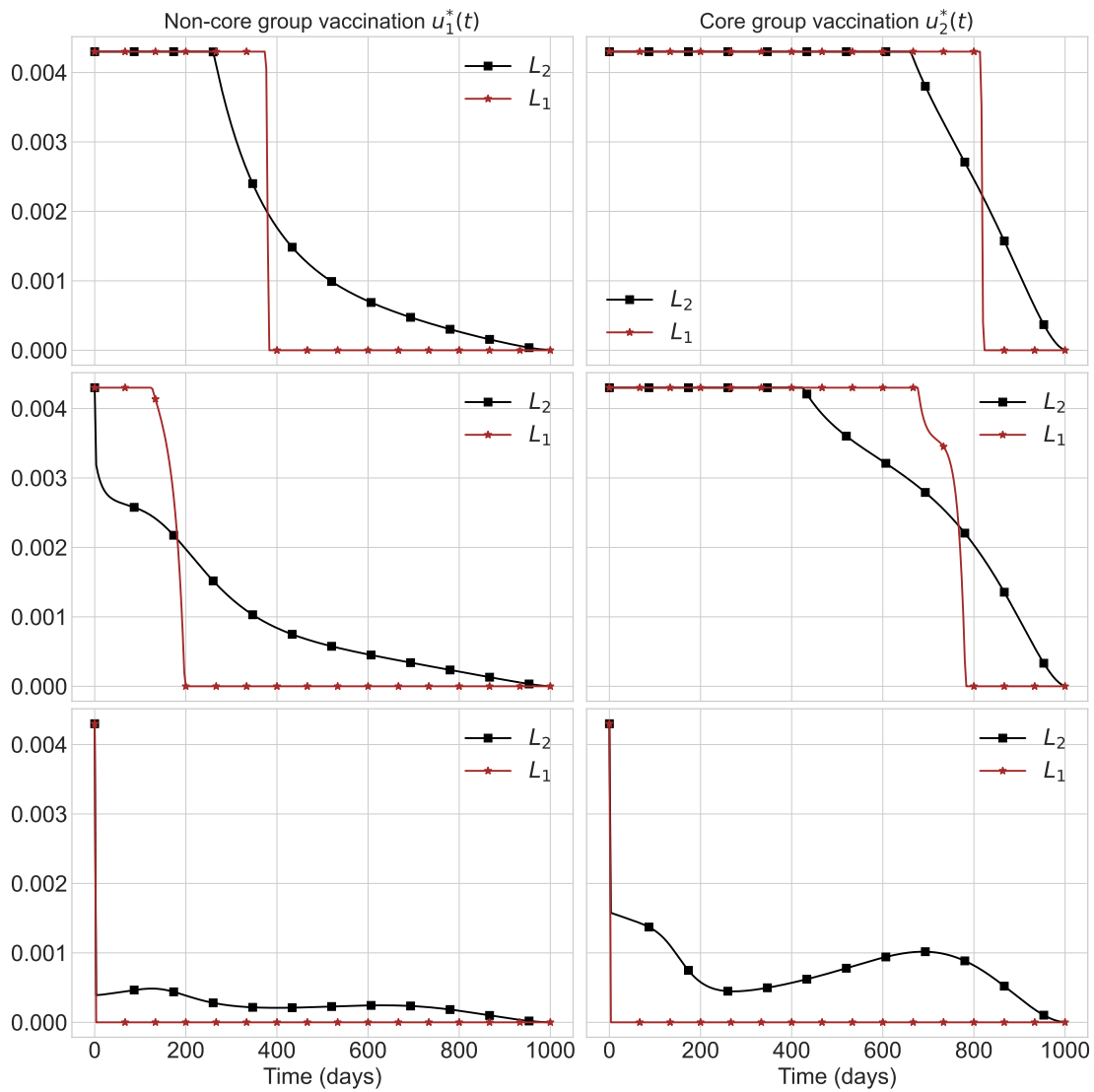


Figure 3: Vaccination rates $u_1^*(t)$ for the non-core group (first column) and the core group $u_2^*(t)$. Row i shows the solution for Case i ($i = I, II, III$). Each plot presents the optimal control profiles for both the L_1 - and the L_2 -formulation.

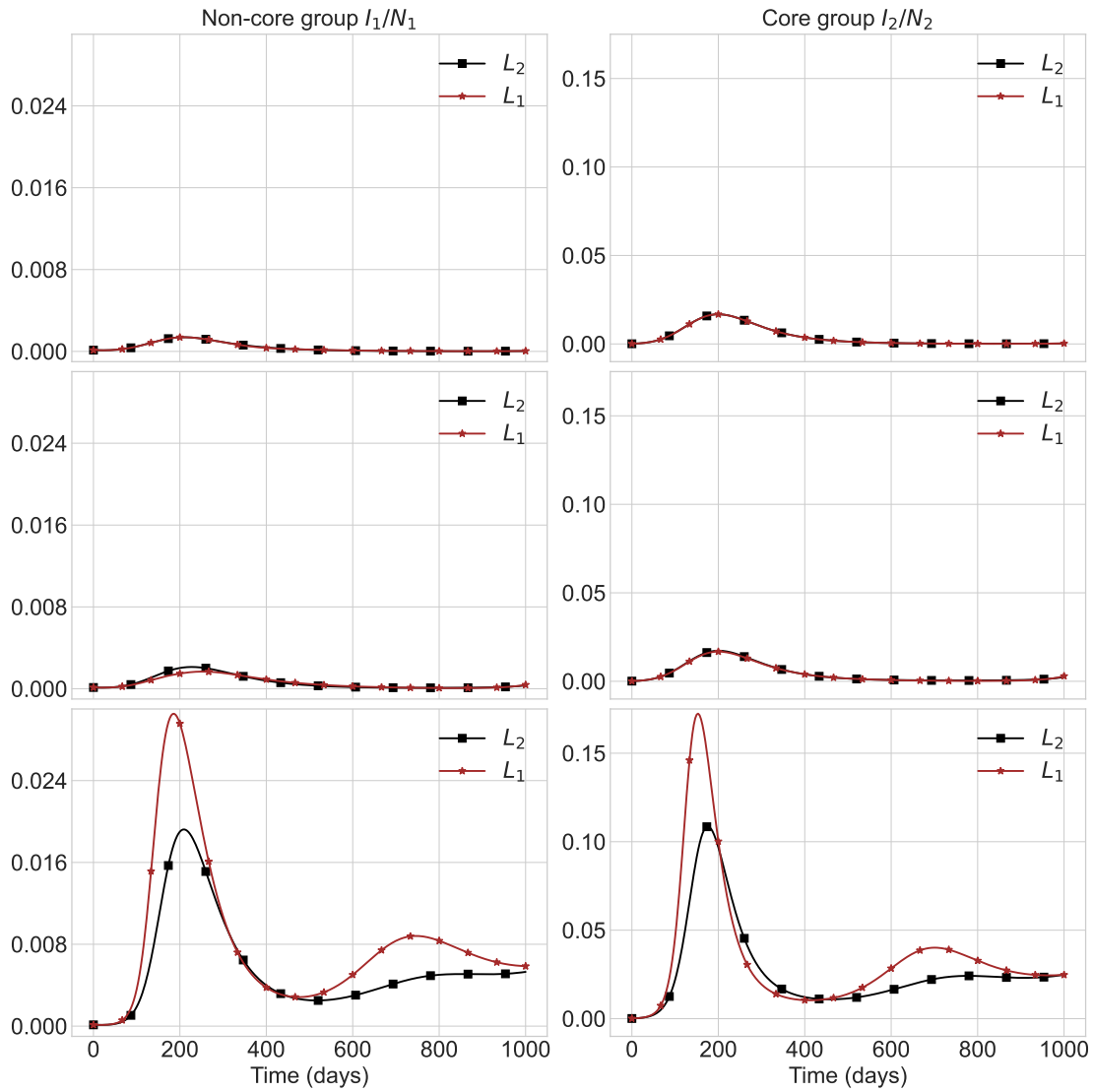


Figure 4: Associated infectious classes of the model (4) corresponding to the vaccination rates presented in Figure 3. The dynamics of the non-core and core groups are shown in the first and second columns, respectively. Row i shows the solution for Case i ($i = I, II, III$). Each plot presents the states for both the L_1 - and the L_2 -formulation.

for less time than the L_1 -control profiles but the L_2 -controls are gradually reduced to zero at the end of the time interval. Similar dynamics are observed for case II (second row in Figure 3) but this time the vaccination rates are maintained for less time due to the increase in the value of the weights and the L_1 -solution presents a singular arc. Overall, the total number of vaccines given for both formulations is very close and the L_2 -control follows the same qualitative properties of the L_1 -control. Furthermore, the associated infectious classes are practically the same for both formulations and each case (see the first and second rows in Figure 4 for case I and case II, respectively). In contrast, for case III the behavior of the control profiles (third row in Figure 3) and the associated infectious classes (third row in Figure 4) differ significantly. As a matter of fact, the optimal control for the L_1 -formulation is not to vaccinate any group at all. Correspondingly, the infectious classes follow practically the same dynamics as in the no-control case (see Figure 1 (b)). Whereas the L_2 -control suggests vaccinating both groups but at lower doses with non-monotone behavior so the vaccination rates decrease the presence of infected individuals in comparison with the no-control case but not enough to eradicate the infection as in cases I and II.

5 Discussion

The choice of the objective functional in optimization problems coming from biomedical and epidemiological applications plays a key role in optimal control outcomes. Nevertheless, in several real-life applications, the actual form of the cost and their dependency on the controls can be uncertain or at least difficult to be defined with an acceptable degree of accuracy. As a result, proposing an appropriate functional form for the objective is a major and habitual challenge in optimal control applications [11, 16, 20, 26, 43]. From a mathematical point of view, it is essential to investigate the robustness and reliability of the outcome with respect to perturbations in the functional form of the objective. Although there are already some advances in the theory of robustness for OCPs much remains to be understood and the relevance of potential applications urges us to explore this problem further [40].

In this paper, we explored the impact of the objective functional on the structure of the optimal control and associated optimal states for a compartmental epidemic model. Specifically, a two-group Kermack-McKendrick-type model where the contact network only includes one non-core and one core group is proposed as a parsimonious approach to consider heterogeneity in the spread of an STI. The so-called preferential mixing governs contact patterns in the model as an improvement over the commonly used homogeneous mixing. The OCT is used to investigate the optimal targeted immunization program to reduce the spread of the infection while minimizing the total vaccine deployment. We formulate an OCP that considers both an L_2 -type objective in which the control cost is postulated to be proportional to a sum of the squares of the considered controls and an L_1 -type objective with a linear dependence on the control. For biological systems the L_1 -formulation is usually preferred from a modeling perspective in the sense that leads to a more realistic interpretation of the cost whereas the L_2 -formulation is more amenable to mathematical analysis and facilitates the numerical approximation of the optimal control solution [16, 26, 43]. Besides the choice of the functional form for the objective, the weight parameters should be properly calibrated to balance the presence of undesirable state variables and the use of control. If the value of the control weights is too high the costs of the intervention usually limit in excess the use of control, and no control will be applied. On the other hand, if the value of the control weights is too low, the optimal control normally suggests the use of control at the maximum rate for long periods of time. The properties of the optimal control solution are hence investigated for a practical range of weight parameters.

For the scenarios explored in this work, the optimal vaccination policy for both the L_1 - and the L_2 -formulation share one important qualitative property, that is, immunization of the core group should be prioritized by policymakers to achieve a fast reduction of the epidemic. However, quantitative aspects of this result can be significantly affected depending on the objective weightings. Overall, our results suggest that the optimal control profiles are reasonably robust with respect to the L_1 - or L_2 -formulation when the monetary cost of the vaccination policy is substantially lower than the morbidity cost associated with the reduction in health and well-being i.e. the cost of infection. Nevertheless, if this is not the case the optimal control profiles can be radically different for each formulation. Furthermore, extra care should be put to select appropriate weights when considering both linear and quadratic control terms. For instance, in model (4) the vaccination rates satisfy $0 \leq u_i^2 \leq u_i \leq u_{max} < 1$ ($i = 1, 2$). Therefore, in this case, L_1 -cost is proportionally more

penalizing than L_2 -cost, and selecting the same weights for both formulations results in radically different behavior in the optimal control solution for each formulation. In many epidemiological scenarios the monetary costs of a healthcare intervention, such as a vaccination program, are usually small in comparison with the potential losses that an epidemic might inflict. For instance, several studies have found that COVID-19 vaccination programs were economically efficient and reduced the overall healthcare costs compared with a scenario without vaccines even with conservative estimates of vaccine effectiveness and high vaccination costs e.g. [2, 31, 32, 33, 47]. Under these conditions, our research suggests that the optimal control results obtained for the classical L_2 -formulation are still able to provide useful information and aid decision-making for many epidemiological settings. Nevertheless, we must remark again that this result is only valid if the intervention cost is clearly lower than the economic cost of illness.

While we examined optimizing objective functionals with either purely L_1 or L_2 control costs, a hybrid formulation incorporating both can also provide a realistic representation of the relationship between vaccination coverage and actual costs in many scenarios. For example, nonlinear forms of control costs are expected to occur if there is an overload in the healthcare system. With a hybrid $L_1 - L_2$ objective, combinations of bang-bang (discrete) and continuous controls are possible and may achieve greater health benefits (e.g. infections averted) at lower overall costs than either pure L_1 or L_2 policies. Hence, investigating the properties of hybrid $L_1 - L_2$ objectives is an important avenue for future research but always bearing in mind that the exponents in the objective can have an uncertain biological interpretation and should be chosen appropriately to achieve an optimal control structure that is feasible to be applied in practice.

Competing interests

The authors declare they have no known competing financial interests that could have appeared to influence the results reported in this work.

CRedit author statement

Fernando Saldaña: Conceptualization, Methodology, Software, Formal analysis, Writing - Original Draft. Amira Kebir: Conceptualization, Formal analysis, Validation, Writing - Review & Editing. José Ariel Camacho-Gutierrez: Software, Formal analysis, Writing - Review & Editing. Maíra Aguiar: Conceptualization, Validation, Supervision, Writing - Review & Editing.

Funding

This research is supported by the Basque Government through BERC 2022-2025 program and by the Spanish Ministry of Sciences, Innovation, and Universities: BCAM Severo Ochoa accreditation CEX2021-001142-S / MICIN / AEI / 10.13039/501100011033. JACG acknowledges support from UABC internal project 400/2936 and financial support from UABC-PREDEPA.

References

- [1] Angulo, M. T., Castaños, F., Moreno-Morton, R., Velasco-Hernández, J. X., and Moreno, J. A. (2021). A simple criterion to design optimal non-pharmaceutical interventions for mitigating epidemic outbreaks. *Journal of the Royal Society Interface*, 18(178):20200803.
- [2] Antonini, M., Eid, M. A., Falkenbach, M., Rosenbluth, S. T., Prieto, P. A., Brammli-Greenberg, S., McMeekin, P., and Paolucci, F. (2022). An analysis of the covid-19 vaccination campaigns in france, israel, italy and spain and their impact on health and economic outcomes. *Health Policy and Technology*, 11(2):100594.
- [3] Bajiya, V. P., Bugalia, S., Tripathi, J. P., and Martcheva, M. (2022). Deciphering the transmission dynamics of covid-19 in india: optimal control and cost effective analysis. *Journal of Biological Dynamics*, 16(1):665–712.

- [4] Balderrama, R., Peressutti, J., Pinasco, J. P., Vazquez, F., and Vega, C. S. d. l. (2022). Optimal control for a sir epidemic model with limited quarantine. *Scientific Reports*, 12(1):12583.
- [5] Bolzoni, L., Della Marca, R., and Groppi, M. (2021). On the optimal control of sir model with erlang-distributed infectious period: isolation strategies. *Journal of Mathematical Biology*, 83:1–21.
- [6] Camacho, A., Díaz-Ocampo, E., and Jerez, S. (2022). Optimal control for a bone metastasis with radiotherapy model using a linear objective functional. *Mathematical Modelling of Natural Phenomena*, 17:32.
- [7] Camacho, A., Saldaña, F., Barradas, I., and Jerez, S. (2019). Modeling public health campaigns for sexually transmitted infections via optimal and feedback control. *Bulletin of mathematical biology*, 81(10):4100–4123.
- [8] Chow, L., Fan, M., and Feng, Z. (2011). Dynamics of a multigroup epidemiological model with group-targeted vaccination strategies. *Journal of Theoretical Biology*, 291:56–64.
- [9] de Los Reyes, A. A. and Kim, Y. (2022). Optimal regulation of tumour-associated neutrophils in cancer progression. *Royal Society Open Science*, 9(2):210705.
- [10] de Pillis, L. G., Gu, W., Fister, K. R., Head, T., Maples, K., Murugan, A., Neal, T., and Yoshida, K. (2007). Chemotherapy for tumors: An analysis of the dynamics and a study of quadratic and linear optimal controls. *Mathematical Biosciences*, 209(1):292–315.
- [11] Engelhart, M., Lebiedz, D., and Sager, S. (2011). Optimal control for selected cancer chemotherapy ode models: a view on the potential of optimal schedules and choice of objective function. *Mathematical biosciences*, 229(1):123–134.
- [12] Fleming, W. and Rishel, R. (1975). *Deterministic and stochastic optimal control*. Springer.
- [13] Gao, S., Martcheva, M., Miao, H., and Rong, L. (2021). A dynamic model to assess human papillomavirus vaccination strategies in a heterosexual population combined with men who have sex with men. *Bulletin of Mathematical Biology*, 83(1):1–36.
- [14] Glasser, J., Feng, Z., Moylan, A., Del Valle, S., and Castillo-Chavez, C. (2012). Mixing in age-structured population models of infectious diseases. *Mathematical Biosciences*, 235(1):1–7.
- [15] Gonzalez-Parra, G., Díaz-Rodríguez, M., and Arenas, A. J. (2020). Mathematical modeling to design public health policies for chikungunya epidemic using optimal control. *Optimal Control Applications and Methods*, 41(5):1584–1603.
- [16] Grigorieva, E., Khailov, E., and Korobeinikov, A. (2018). Optimal control for an seir epidemic model with nonlinear incidence rate. *Studies in Applied Mathematics*, 141(3):353–398.
- [17] Haddad, G., Kebir, A., Raissi, N., Bouhali, A., and Miled, S. B. (2022). Optimal control model of tumor treatment in the context of cancer stem cell. *Mathematical Biosciences and Engineering*, 19(5):4627–4642.
- [18] Heffernan, J. M., Lou, Y., Steben, M., and Wu, J. (2014). Cost-effectiveness evaluation of gender-based vaccination programs against sexually transmitted infections. *Discrete & Continuous Dynamical Systems-B*, 19(2):447.
- [19] Hethcote, H. W. and Yorke, J. A. (1984). *Gonorrhoea transmission dynamics and control*, volume 56. Springer-Verlag, Berlin, Germany.
- [20] Igoe, M., Casagrandi, R., Gatto, M., Hoover, C. M., Mari, L., Ngonghala, C. N., Remais, J. V., Sanchirico, J. N., Sokolow, S. H., Lenhart, S., et al. (2023). Reframing optimal control problems for infectious disease management in low-income countries. *Bulletin of Mathematical Biology*, 85(4):31.
- [21] Jacquez, J. A., Simon, C. P., Koopman, J., Sattenspiel, L., and Perry, T. (1988). Modeling and analyzing hiv transmission: the effect of contact patterns. *Mathematical Biosciences*, 92(2):119–199.

- [22] Kamien, M. I. and Schwartz, N. L. (2012). *Dynamic optimization: the calculus of variations and optimal control in economics and management*. courier corporation.
- [23] Kim, S., Jung, E., et al. (2018). Mathematical model and intervention strategies for mitigating tuberculosis in the philippines. *Journal of theoretical biology*, 443:100–112.
- [24] Krener, A. J. (1977). The high order maximal principle and its application to singular extremals. *SIAM Journal on Control and Optimization*, 15(2):256–293.
- [25] Ledzewicz, U., Naghnaeian, M., and Schättler, H. (2012). Optimal response to chemotherapy for a mathematical model of tumor–immune dynamics. *Journal of mathematical biology*, 64:557–577.
- [26] Ledzewicz, U. and Schättler, H. (2020). On the role of the objective in the optimization of compartmental models for biomedical therapies. *Journal of optimization theory and applications*, 187:305–335.
- [27] Lenhart, S. and Workman, J. T. (2007). *Optimal control applied to biological models*. Crc Press.
- [28] Lindau, S. T. and Gavrilova, N. (2010). Sex, health, and years of sexually active life gained due to good health: evidence from two us population based cross-sectional surveys of ageing. *BMj*, 340.
- [29] Lukes, D. L. (1982). *Differential equations: classical to controlled*. Elsevier.
- [30] Miller Neilan, R. L., Schaefer, E., Gaff, H., Fister, K. R., and Lenhart, S. (2010). Modeling optimal intervention strategies for cholera. *Bulletin of mathematical biology*, 72:2004–2018.
- [31] Padula, W. V., Malaviya, S., Reid, N. M., Cohen, B. G., Chingcuanco, F., Ballreich, J., Tierce, J., and Alexander, G. C. (2021). Economic value of vaccines to address the covid-19 pandemic: a us cost-effectiveness and budget impact analysis. *Journal of Medical Economics*, 24(1):1060–1069.
- [32] Reddy, K. P., Fitzmaurice, K. P., Scott, J. A., Harling, G., Lessells, R. J., Panella, C., Shebl, F. M., Freedberg, K. A., and Siedner, M. J. (2021). Clinical outcomes and cost-effectiveness of covid-19 vaccination in south africa. *Nature communications*, 12(1):6238.
- [33] Richards, F., Kodjamanova, P., Chen, X., Li, N., Atanasov, P., Bennetts, L., Patterson, B. J., Yektashenas, B., Mesa-Frias, M., Tronczynski, K., et al. (2022). Economic burden of covid-19: a systematic review. *ClinicoEconomics and Outcomes Research*, pages 293–307.
- [34] Saldaña, F. and Barradas, I. (2018). Control strategies in multigroup models: the case of the star network topology. *Bulletin of mathematical biology*, 80(11):2978–3001.
- [35] Saldaña, F., Camacho-Gutiérrez, J. A., Villavicencio-Pulido, G., and Velasco-Hernández, J. X. (2022). Modeling the transmission dynamics and vaccination strategies for human papillomavirus infection: An optimal control approach. *Applied Mathematical Modelling*, 112:767–785.
- [36] Saldaña, F., Korobeinikov, A., and Barradas, I. (2019). Optimal control against the human papillomavirus: protection versus eradication of the infection. In *Abstract and applied analysis*, volume 2019. Hindawi.
- [37] Saldaña, F., Steindorf, V., Srivastav, A. K., Stollenwerk, N., and Aguiar, M. (2023). Optimal vaccine allocation for the control of sexually transmitted infections. *Journal of Mathematical Biology*, 86(5):75.
- [38] Saldaña, F. and Velasco-Hernández, J. X. (2021). Modeling the covid-19 pandemic: a primer and overview of mathematical epidemiology. *SeMA Journal*, pages 1–27.
- [39] Schättler, H., Ledzewicz, U., and Maurer, H. (2014). Sufficient conditions for strong local optimality in optimal control problems with l2-type objectives and control constraints. *Discrete & Continuous Dynamical Systems-Series B*, 19(8).
- [40] Schättler, H. M., Ledzewicz, U., and Cardwell, B. (2011). *Robustness of optimal controls for a class of mathematical models for tumor anti-angiogenesis*. American Institute of Mathematical Sciences.

- [41] Sepulveda-Salcedo, L. S., Vasilieva, O., and Svinin, M. (2020). Optimal control of dengue epidemic outbreaks under limited resources. *Studies in Applied Mathematics*, 144(2):185–212.
- [42] Sharbayta, S. S., Buonomo, B., d’Onofrio, A., and Abdi, T. (2022). ‘period doubling’ induced by optimal control in a behavioral sir epidemic model. *Chaos, Solitons & Fractals*, 161:112347.
- [43] Sharp, J. A., Browning, A. P., Mapder, T., Baker, C. M., Burrage, K., and Simpson, M. J. (2020). Designing combination therapies using multiple optimal controls. *Journal of Theoretical Biology*, 497:110277.
- [44] Srivastav, A. K., Steindorf, V., Stollenwerk, N., and Aguiar, M. (2023). The effects of public health measures on severe dengue cases: An optimal control approach. *Chaos, Solitons & Fractals*, 172:113577.
- [45] Tchoumi, S., Diagne, M., Rwezaura, H., and Tchuenche, J. (2021). Malaria and covid-19 co-dynamics: A mathematical model and optimal control. *Applied mathematical modelling*, 99:294–327.
- [46] Wächter, A. and Biegler, L. T. (2006). On the implementation of an interior-point filter line-search algorithm for large-scale nonlinear programming. *Mathematical programming*, 106:25–57.
- [47] Wang, W.-C., Fann, J. C.-Y., Chang, R.-E., Jeng, Y.-C., Hsu, C.-Y., Chen, H.-H., Liu, J.-T., and Yen, A. M.-F. (2021). Economic evaluation for mass vaccination against covid-19. *Journal of the Formosan Medical Association*, 120:S95–S105.
- [48] Zhou, Y., Yang, K., Zhou, K., and Liang, Y. (2014). Optimal vaccination policies for an sir model with limited resources. *Acta biotheoretica*, 62:171–181.